Assessment of a bolted-flange connection for ITER Test Blanket Module

Tony Zaouter, Karl Vulliez, Benjamin Michel, Stéphane Gazzotti, Jean-Pierre Friconneau, Jean-Pierre Martins

HAL Id: cea-03142659

https://cea.hal.science/cea-03142659

Submitted on 16 Feb 2021

Assessment of a bolted-flange connection for ITER Test Blanket Module

T. Zaouter[a,*], K. Vulliez[a], B. Michel[a], S. Gazzotti[b], J.-P. Friconneau[b], J.-P. Martins[c]

[a]*CEA, DES, ISEC, DE2D, SEAD, Laboratoire d'Étanchéité, Univ. Montpellier, Marcoule, France.*
[b]*CEA Cadarache, IRFM, F-13108 Saint-Paul-lez-Durance, France.*
[c]*ITER Organization, Route de Vinon-sur-Verdon, 13067 Saint-Paul-lez-Durance, France.*

Abstract

In ITER, the 'Pipe Forest (PF)' is a network of pipes that connects the Ancillary Equipment Unit to the Test Blanket Module (TBM) at the level of the equatorial port-plug of the reactor prototype. The goal of ITER's TBM program is to validate concepts to be adopted for the DEMO tritium Breeding Blankets. Different types of pipes are mounted on the port-plug among which those used for cooling or tritium processing. During plasma operation, the PF has to accommodate severe thermomechanical loads. It shall also provide protection from abnormal contamination and be designed to ease connection/disconnection operations. With numerical simulation, this work assesses the use of bolted flanges as an alternative to the welded solution to connect the PF on the TBMs inside the port cell environment. The proposed designs integrate metallic seals as well as an embedded cooling system in the flanges when necessary, to limit the temperature of the seals and the bolts and prevent irreversible damage. It is shown that bolted-flange junctions for the PF are a credible solution. Still, important stresses in the socket of the flanges are present but do not represent a problematic issue for dimensioning purposes, as they shall be accommodated with a small amount of plastic strain.

Keywords: Bolted-flange, Numerical Simulation, ITER, Test Blanket Module, Pipe Forest

1. Introduction

The goal of the ITER Test Blanket Module (TBM) program is to test and validate concepts to be adopted for the DEMO tritium Breeding Blankets. These modules will be placed at the level of the equatorial port-plug of ITER (two of them are present in each port-plug) [1, 2]. The concepts use different pipes dedicated to cooling (water and/or helium), tritium process (liquid lithium-lead alloy as a breeder or tritium extraction with helium purge gas) and neutronic activation diagnostics in the port cell. These fluids are driven through a network of pipes called 'Pipe Forest (PF)', connecting the Ancillary Equipment Unit to the two TBMs. The pipes constituting this network have a loop shape design so as to remain relatively flexible, since the PF will have to accommodate important thermal expansion and mechanical displacements during plasma operation. The PF shall also provide protection from abnormal contamination and be compatible with the TBM program requiring several replacements and therefore connection/disconnection operations. In this regards, the connection of the PF on the TBM inside the constrained port cell environment should be conceived under the principles of the 'ALARA' approach [3], ideally involving remote or hands-on maintenance steps. Thereby, the use of bolted flanges as a potential alternative to a welded connection is evaluated in this article. To this day, no

particular technical solution is preferred and both need to be examined. The welded solution appears more classical at first hand, but the maintenance and welding quality control might involve potentially tedious operations in the constrained port cell environment. Moreover, the welding of some materials as Eurofer for PF applications still needs investigations. On the other hand, the bolted-flange solution would facilitate maintenance operations a priori, at the expense of adding significant mass on the pipes and taking more space in the PF.

We focus our attention on three particular pipes, namely helium, water and liquid lithium-lead alloy pipes, for which flange designs and modelling hypotheses are proposed in Sec. 2. The capabilities of the suggested designs to sustain the external applied loads and thermal constraints are assessed by numerical simulations using ABAQUS® and whose results are presented and discussed in depth in Sec. 3. Finally, Sec. 4 gives the conclusions and perspectives for this study.

2. Mechanical design and numerical model

2.1. Preliminary considerations

The main function of a bolted-flange connection is to ensure the confinement of the conveyed fluid inside the pipe. For the preliminary design phase presented in this work, we concentrate on three fluid lines of the PF (lithium-lead, water and helium) with different mechanical constraints and thermodynamic conditions, summarised in

---

	Lithium-Lead	Water	Helium
Pipe size	DN25	DN65	DN80
Pipe material	Eurofer	SS-316L	SS-316L
Outer diam. [mm]	33.7	76.1	88.9
Thickness [mm]	5	12.5	8.8
Flange 'Class'	300	2,500	2,500
Bolts	4×M16	8×M30	18×M24
Bolt tension [kN]	20	30	60
Temperature [°C]	340	345	525
Pressure [MPa]	0.9	18.8	9.8
Traction [N]	1,000	3,025	1,930
Bending [N·m]	325	2,975	7,175
Torsion [N·m]	100	850	2,685

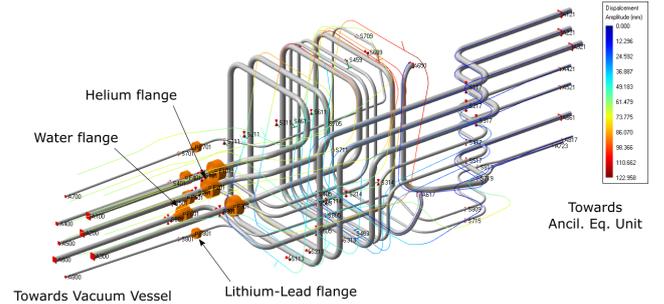Table 1: Summary of the design properties for the three flanges.

Figure 1: Model of the pipes of the PF considered for the dynamical analysis in DST PipeStress. The computed deformed configuration in the case of SL2 seismic event is superimposed. The position of the three flanges studied in this article are indicated.

Tab. 1 (to which continuous reference will be made in the remainder of this article). For these flanges the leak rate criterion has to be defined in accordance with the specified requirements and operating conditions. In the case of liquids (lithium-lead, water) a rather crude gaseous equivalent leak rate criterion ('bubble tight') with a single metallic seal (HELICOFLEX® for example) is proposed. On the other hand, for gases (pure helium or a mix of helium and tritium), a more stringent criterion is suggested ('helium tight'). In addition, for these systems, a leak surveillance system is proposed requiring a double torus metallic seal to monitor the leak in its inner volume. This will induce supplementary mechanical constraints on the assembly (roughly a doubling of the tightening effort). With operating temperature below 400 °C for water and lithium-lead, standard bolted flanges taken from the industrial norm [4] can be implemented. However, for the helium pipe, temperature higher than 400 °C and important tension in the fasteners can lead to serious creep effects leading to an unloading of the seals and leakage of the assembly. To prevent such consequence, it is recommended to integrate water cooling in the flanges close to the bolts and the seals to limit their temperature. We close this preamble saying that the flanges will be thermally insulated and rotatable to compensate the possible misalignments. Furthermore, the dimensions of the pipes are imposed by a companion work following the norm [5] and the loads on the flanges result from the post-processing of a dynamical analysis of the PF with the DST PipeStress software according to the RCC-MRx [6]. Basically, the pipes are represented by linear elastic beams comprising straight parts, elbows and fittings, and the flanges are included as analogous rigid bodies with equivalent mass. Then, the loadings considered on the PF for the analysis are the sustained dead weight and dynamical loads, thermal expansion and anchor displacements. As an example, Fig. 1 shows the computed displacements of the pipes in the conservative case of an SL2 seismic event (accidental conditions).

2.2. Water & Lithium-Lead flanges

Considering the thermodynamic conditions and materials given in Tab. 1, the design of the water and lithium-lead flanges is based solely on the norm [4]. The 'Class' of each flange is chosen in accordance. The obtained design of the water assembly is shown on Fig. 2a, that of the lithium-lead flange being highly similar. In this figure, the HELICOFLEX® metal seal is integrated as a analogous 'gasket element' whose load-compression behaviour (shown in Fig. 3) is obtained apart by fine-scale finite element simulations (see [7] for a detailed description of the model used). For the water flange, a seal of diameter 90.5 mm and silver liner is used, while for the lithium-lead flange, a seal of diameter 43 mm and pure iron liner is employed. The resulting approximate mass of each bolted-flange assembly is 45 kg and 4 kg for water and lithium-lead respectively. Since no cooling of the flanges is necessary, a linear elastic static analysis is performed at constant temperature of the assembly. The material properties for the flanges (identical to that of the pipes) and the bolts (ASTM SA-540 B21 Class 1 steel) are found in [6] and [8] respectively. Regarding the boundary conditions, one end of the pipe is blocked (except radial displacements), and bolt tension is applied to compress the seal. Concentrated traction force, bending and torsion moments are then exerted at the other end of the pipe. Finally, pressure in the pipe and temperature are applied.

2.3. Helium flange

A custom design is required for the helium assembly that integrates water cooling. It is based on a 'Class 2,500' standard flange [4]. The concept is presented on Fig. 2b and a technical drawing is given in Appendix A. As can be seen, the double-torus HELICOFLEX® seal (silver liner, mean diameter 205 mm, behaviour in Fig. 3) is placed farthest away from the pipe filled with hot helium, and the water cooling channels are located in both flanges above the seal to limit its temperature. This will cool down the bolts located nearby as well. Compared to the norm, more bolts with smaller cross section are integrated to ensure a more homogeneous compression of the seal. Direct contact
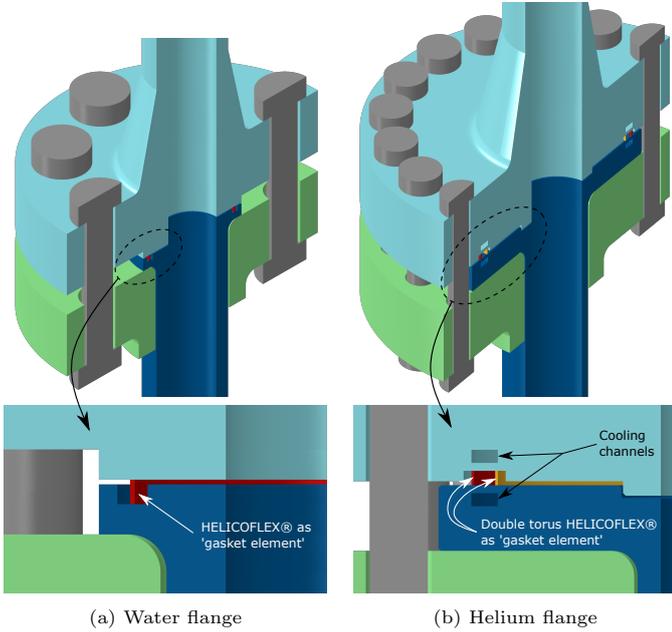
(a) Water flange   (b) Helium flange

Figure 2: Simplified view of water and helium flanges (half model shown).
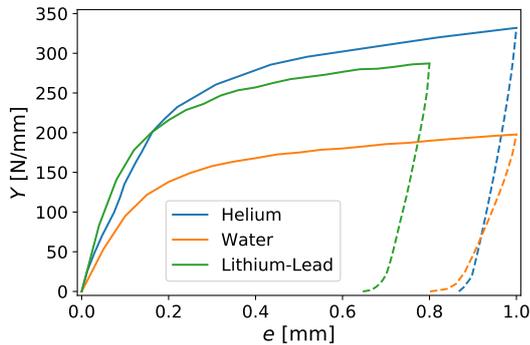

Figure 3: Individual characteristic curves of the three HELICOFLEX® seals giving the linear load as a function of the seal compression. Solid line: compression curve; dashed line: unloading curve.

between the two flanges is expected on the socket close to the inner surface of the pipe, far from the seal, to hinder contact heat transfer near this latter and ease the cooling. The resulting mass of the assembly is approximately 80 kg. The boundary conditions and the procedure to apply the mechanical loads are identical to that described in Sec. 2.2. However, fully-coupled thermomechanical simulations will be performed for the helium assembly and this needs supplementary assumptions. First, thermal contact conductance is required to quantify the heat transfer through contacts. A temperature- and contact pressure-dependant global value for steel-steel contacts is taken following the Mikić elastic theory [9], assuming a root mean square (RMS) surface roughness of 1.2 μm. At the seal-flange interface, a constant value of $15 \text{ kW} \cdot \text{m}^{-2} \cdot \text{K}^{-1}$ for the thermal contact conductance is utilised, and shall be regarded as an apparent contact heat transfer coefficient between the whole seal and the steel flanges. This value is based on our own experimental experience on real bolted flange assemblies. It remains quite constant around the nominal compression of the seal and for small unloading, due to the elastic recovery capabilities of the seal allowing to maintain an intimate plastic contact at the roughness level. This value is rather conservative and appears sufficient for a pre-design phase. Secondly, convective heat transfer is supposed to take place in the pipe and the cooling channels. This coefficient can be calculated as:

$$h_c = \text{Nu} \frac{\lambda_f}{D_h} \tag{1}$$

with λ_f the thermal conductivity of the fluid, D_h the hydraulic diameter of the duct and Nu the Nusselt number which, for turbulent forced convection, is given by the Colburn relation [10] as a function of the Reynolds and Prandtl numbers as:

$$\text{Nu} = 0.023 \, \text{Re}^{0.8} \text{Pr}^{0.333} \tag{2}$$

For the gaseous helium in the pipe, assuming a mass flow rate of $1.4 \text{ kg} \cdot \text{s}^{-1}$ at 525 °C and taking the various fluid properties from [11], we obtain $h_c^0 = 1{,}115 \text{ W} \cdot \text{m}^{-2} \cdot \text{K}^{-1}$. Similarly, for the cooling channels with design dimensions of Fig. A.7, assuming a water velocity of $2 \text{ m} \cdot \text{s}^{-1}$ at 34 °C and 1 MPa, and using the physical properties given in [12], we obtain $h_c^1 = 9{,}280 \text{ W} \cdot \text{m}^{-2} \cdot \text{K}^{-1}$. Since water velocity is a design hypothesis, this choice and its influence on the value of h_c^1 will be examined thereafter around these nominal conditions.

3. Results

3.1. Water & Lithium-Lead flanges

We first present the results obtained for the water and lithium-lead assemblies. Fig. 4 shows the computed fields of equivalent Tresca stress in both assemblies and Tab. 2 summarises some results at particular locations of interest, namely the maximum stresses in the assembly, in the

bolts and in the pipes (far from the flanges). In both cases, the maximum stress in the assembly is obtained at the socket of the bottom flange close to the groove of the seal. For the water flange, this maximum stress is higher than the yield stress of SS-316L at the considered temperature ($R_{p0.2} = 101$ MPa), the same goes for the stress in the pipes. For the lithium-lead flange, the equivalent stress is always smaller than the yield stress of Eurofer at given temperature ($R_{p0.2} = 423$ MPa) so this poses no dimensioning issue at first hand. As expected, the maximum stress in the bolts is also much smaller than the corresponding yield strength at 340 °C ($R_{p0.2} = 880$ MPa).

Naturally, the pre-designs considered in this article should comply with the RCC-MRx [6] design code for the ITER machine and solely monitoring an equivalent stress in the assembly is not sufficient to assess the validity of a design. Namely, stress linearisation should be performed at various locations in the assemblies (shown as red lines on Fig. 4) to deduce a membrane (σ_m) and a bending stress (σ_b). In the flanges, these values shall fulfil the design criterions $\sigma_m < S_m$ and $\sigma_m + \sigma_b < 1.5 S_m$ where S_m is the maximal admissible stress of the material. For SS-316L around 345 °C, we have $S_m = 103$ MPa; for Eurofer we have $S_m = 185$ MPa. For the tensioners, the membrane and bending stresses might be evaluated through the middle cross section of the most constrained one and further compared to the maximum admissible stress for bolting materials S_{mB} as $\sigma_m < 2 S_{mB}$ and $\sigma_m + \sigma_b < 3 S_{mB}$. To remain conservative, we take $S_{mB} = 287$ MPa corresponding to $R_{p0.2}/3$ at the maximum temperature allowed for the bolting material (375 °C [6, 8]). Tab. 3 presents the linearised stresses at the particular locations in the assemblies as well as the design margins (in brackets) regarding the previously reported criterions. A positive margin indicates that the corresponding criterion is met while a negative value demonstrates a failure to do so. Overall, comfortable margins can be seen for both flanges and for the bolts demonstrating that the proposed standard designs are acceptable. Though, for the water flange, the membrane stress is slightly higher than admissible in the pipe (P) and at the socket of the bottom flange (F4) where the maximum Tresca stress is located. This remains acceptable as this will be accommodated locally by a small amount of plastic deformation with strain hardening in practice. Therefore it appears non-constraining for a pre-design phase and could be assessed and optimised in more details in future work.

3.2. Helium flange

For the helium assembly, the computed stress and temperature fields for the nominal cooling situation are presented on Fig. 5 with one or both cooling channels activated. Particular values are summarised in Tab. 2. The temperature gradient imposed by the cooling produces important stresses around the socket, above the maximum yield stress. The maximum stress is less important when only one cooling channel is activated, as the
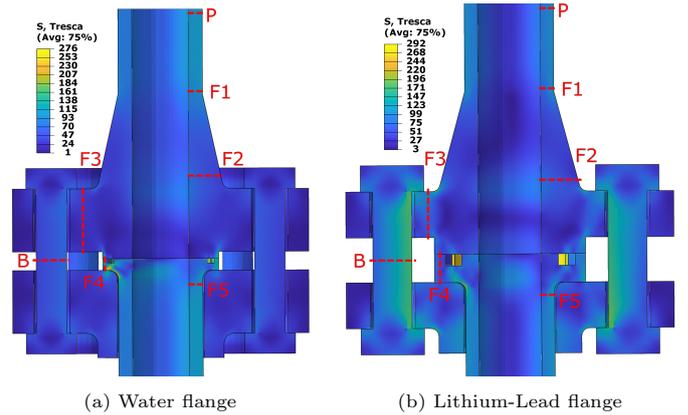

(a) Water flange   (b) Lithium-Lead flange

Figure 4: Computed Tresca equivalent stress (in MPa) for the water and lithium-lead assemblies. The red dashed lines indicate the positions used for stress linearisation.

temperature in the flange with inactive cooling is more homogeneous and thermal strains smaller. The stress in the bolts remains reasonable regarding the temperature, at least when two cooling channels are used. While the temperature in the bolts and the seal is relatively small when both cooling channels are used, providing potential thermal design margins, it becomes unreasonably elevated when using only one cooling channel and could trigger undesired creep effects. This justifies the need for two water cooling channels, and the case of using only one channel will not be further discussed. As in Sec. 3.1, Tab. 3 summarises the membrane and bending stresses at locations provided in Fig. 5a using two cooling channels. The stresses in the bolts present important margins as expected. In the flanges, the analysis following the RCC-MRx code is made more arduous to exploit due to the inhomogeneous temperature field inducing a gradient of material properties. To be conservative the maximal admissible stress $S_m = 89$ MPa at 525 °C was used. Important negative margins can be seen so the design cannot be accepted as is. However, strain hardening might help to accommodate the important stresses without difficulty especially in the flanges considering their massive dimensions. For the pipes this seems more critical and needs to be addressed first in future work. Various options can be envisaged to design a flange which remains in the mechanical limits fixed by the code: i) using Eurofer which has a higher admissible stress than SS-316L; ii) increase the thickness of the pipes; iii) modify the configuration of the helium line in the PF to decrease the mechanical loads.

We now turn our attention on the total heat flux φ that needs to be extracted by the cooling channels. In the nominal configuration studied so far, 3.53 kW are necessary which is relatively important regarding the potential number of flanges to be cooled down in the PF, but still remains reasonable for the proposed design to be acceptable. By varying the water convective heat transfer coefficient down to $h_c^1 = 382$ W·m^{-2}·K^{-1} (corresponding to laminar flow in the channels), the cooling heat flux can

	Lithium-Lead	Water	Helium (2 cool. ch.)	Helium (1 cool. ch.)
$\sigma_{\max}$ [MPa]	250	276	1,340	1,097
σ_{bolt} [MPa]	212	81	383	521
σ_{pipe} [MPa]	107	109	202	203
$T_{\max}$ [°C]	340	345	525	525
T_{bolt} [°C]	–	–	221	361
T_{seal} [°C]	–	–	64	417
T_{channel} [°C]			62	417

Table 2: Summary of some Tresca stresses (σ) and temperatures (T) at different locations of the assemblies.

	Lithium-Lead		Water		Helium	
Location	σ_m [MPa]	$\sigma_m + \sigma_b$ [MPa]	σ_m [MPa]	$\sigma_m + \sigma_b$ [MPa]	σ_m [MPa]	$\sigma_m + \sigma_b$ [MPa]
P	96 (+48%)	108 (+61%)	106 (-3%)	110 (+28%)	195 (-119%)	204 (-52%)
F1	89 (+52%)	113 (+50%)	93 (+10%)	103 (+33%)	184 (-106%)	199 (-49%)
F2	41 (+78%)	83 (+70%)	52 (+50%)	72 (+54%)	75 (+16%)	317 (-136%)
F3	66 (+64%)	87 (+69%)	17 (+84%)	42 (+73%)	307 (-245%)	333 (-149%)
F4	66 (+64%)	71 (+74%)	110 (-7%)	155 (+0%)	148 (-66%)	422 (-215%)
F5	88 (+52%)	160 (+42%)	96 (+7%)	114 (+26%)	311 (-249%)	481 (-259%)
B	120 (+74%)	179 (+74%)	52 (+89%)	68 (+90%)	161 (+65%)	258 (+62%)

Table 3: Summary of the membrane (σ_m) and membrane plus bending ($\sigma_m + \sigma_b$) linearised stresses at some locations in the assemblies. In parenthesis are the corresponding design margins.

be reduced to 2.39 kW, which remains important because convective transfer on the helium side is significant. Results for intermediate values of h_c^1 are compiled in the first four rows of Tab. 4 and as blue dots on Fig. 6. In all cases the maximal temperature of the bolts and seals was of 314 °C and the maximal stress was relaxed compared to the nominal configuration, which is acceptable as a design. As a general observation, lowering convection reduces the stresses but in the range investigated, the margins regarding membrane and bending stresses remain of the same order as that of Tab. 3, therefore it does not help in making a design mechanically acceptable for the code at first order. Additional simulations were performed conjointly varying h_c^0 and h_c^1 to explore the cooling capabilities of the system (last rows of Tab. 4 and red squares on Fig. 6). To qualitatively explain the observed water cooling behaviour of the flanges, a simple model can be developed considering a cylindrical annulus, of thermal conductivity λ_s, submitted to purely convective heat transfer of coefficient h_c^j at its external surfaces located at radius R_j, $j = 0, 1$. Heat flux conservation then reads:

$$\varphi = \frac{2\pi}{\ln(R_1) - \ln(R_0)} \lambda_s (T_0 - T_1)$$
$$= 2\pi R_0 h_c^0 (T_{0\infty} - T_0) = 2\pi R_1 h_c^1 (T_1 - T_{1\infty}) \quad (3)$$

where T_j is the surface temperature at radius R_j and $T_{j\infty}$ the 'sink' temperature at side $j = 0, 1$. Next, defining φ_∞ the 'ideal flux' with perfect convection (i.e., when, $h_c^j \to +\infty$, or equivalently $T_j \to T_{j\infty}$) as:

$$\varphi_\infty = \frac{2\pi}{\ln(R_1) - \ln(R_0)} \lambda_s (T_{0\infty} - T_{1\infty}) \quad (4)$$

a dimensionless heat flux can be further written such that:

$$\frac{\varphi}{\varphi_\infty} = \frac{\text{Bi}}{1 + \text{Bi}} \quad (5)$$

where Bi is the harmonic average Biot number defined as:

$$\frac{1}{\text{Bi}} = \frac{R_1 - R_0}{\ln(R_1) - \ln(R_0)} \left(\frac{1}{R_0 \text{Bi}_0} + \frac{1}{R_1 \text{Bi}_1} \right) \quad (6)$$

with $\text{Bi}_j = h_c^j (R_1 - R_0)/\lambda_s$ the Biot number at the annulus surface j. Considering the estimates $R_0 = 35.7$ mm, $R_1 = 97.5$ mm and $\lambda_s = 20.3 \text{ W} \cdot \text{m}^{-1} \cdot \text{K}^{-1}$, Fig. 6 shows that the simulation data are well represented by the model of Eq. (5). Note that due to the geometric complexity of the assembly, the simple model developed can only provide insight on the variation of the heat flux with convection so that Eq. (4) cannot be used directly and φ_∞ is rather estimated to 5 kW by a fitting of the values in Tab. 4. The harmonic dependence of φ on Bi_1 through Bi in model (5) explains the difficulty in sensibly diminishing the cooling power, even while lowering h_c^1 down to its laminar flow value. Optimisation of the thermal performance of the assembly requires that a compromise be made between the desire to have a minimum temperature for the seal and the fasteners and a minimum extracted heat flux regarding the available cooling capacity. Besides using a lower cooling convection, a modification of the position, size and shape of the cooling channels (to reduce the exchange surface for example) appears a possible way to achieve this objective.

5

h_c^0 $[\text{W} \cdot \text{m}^{-2} \cdot \text{K}^{-1}]$	h_c^1 $[\text{W} \cdot \text{m}^{-2} \cdot \text{K}^{-1}]$	φ $[\text{kW}]$
1,115	9,280	3.53
1,115	3,061	3.37
1,115	845	2.91
1,115	382	2.39
6,115	9,280	4.31
3,115	9,280	4.09
350	382	1.90

Table 4: Cooling heat flux results for different helium and water convection coefficients.
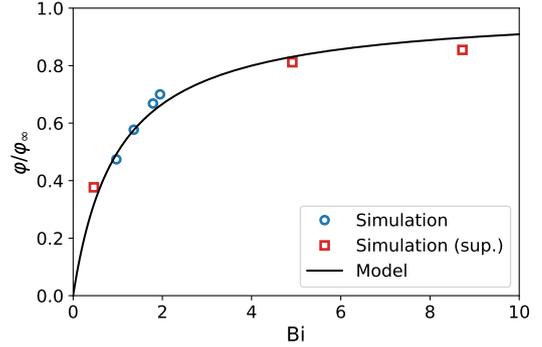

Figure 6: Dimensionless water cooling heat flux as a function of the Biot number of Eq. (6). Blue dots: simulations varying h_c^1; red squares: supplementary simulations varying both h_c^0 and h_c^1; solid line: model of Eq. (5) with $\varphi_\infty = 5$ kW (best fit).

4. Conclusions

Standard industrial bolted-flange designs have been proposed for the water and lithium-lead lines of the PF and an actively cooled custom flange design for a helium line, integrating metallic seals. These designs were assessed by numerical simulations using ABAQUS®. In all cases, locally high elastic stress are present but shall not pose significant design issues as they might be accommodated by a small amount of plastic strain. For the water and lithium-lead assemblies, the proposed designs are compatible with the RCC-MRx design code for ITER. The helium flange could not pass the code requirements as is. Plastic accommodation shall not pose particular trouble in the massive flanges, contrary to the pipes which need design revision beforehand. Moreover, it was shown that water cooling in both flanges was necessary to keep the bolts and the seal at a reasonable temperature (below 400 °C). The necessary cooling power was relatively important but the steady state temperature (see Tab. 2) offers some margins for thermomechanical design optimisation. Bolted-flange connection therefore appears as a potential alternative to the welded solution in the PF.

Though mechanically validated, the flange design for the lithium-lead line might not be totally appropriate in practice, due to potential 'cold spot' issues in the vicinity of the flange. To improve and ease mounting/dismounting of the flanges with hands-on or remote handling operations, potential use of a 'Quick Disconnecting System' instead of a bolted assembly can be thought and remains to be qualified for severe thermodynamics conditions.

Disclaimer

The views and opinions expressed herein do not necessarily reflect those of the ITER Organization.

(a) Stress, 2 cooling channels

(b) Stress, 1 cooling channel

(c) Temp., 2 cooling channels
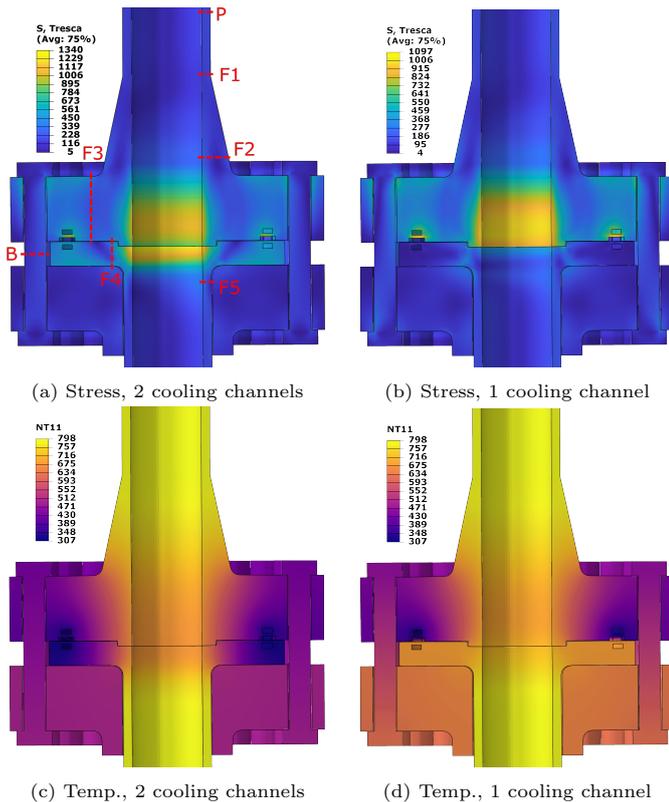
(d) Temp., 1 cooling channel

Figure 5: Computed Tresca equivalent stress (in MPa) and temperature field (in K) for the helium assembly, with one or two cooling channels activated. The red dashed lines indicate the positions used for stress linearisation.
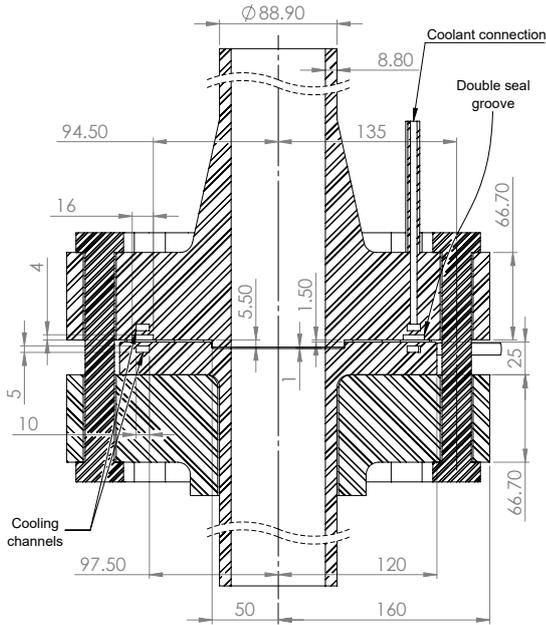
Figure A.7: Cut view of the helium flange assembly.

Acknowledgements

Appendix A. Simplified plan of the helium flange

Fig. A.7 of this appendix presents the plan of the helium flange. Only the custom (non-standard) dimensions are indicated, the remaining ones being taken from the norm [4]. The inlet and outlet connections for the coolant are also represented for the upper flange (indicated), and for the lower flange (visible on the right, between the upper flange and the rotatable flange).

References

[1] L. M. Giancarli, M. Abdou, D. J. Campbell, V. A. Chuyanov, M. Y. Ahn, M. Enoeda, C. Pan, Y. Poitevin, E. Rajendra Kumar, I. Ricapito, Y. Strebkov, S. Suzuki, P. C. Wong, M. Zmitko, Overview of the ITER TBM program, Fusion Engineering and Design 87 (5) (2012) 395–402, tenth International Symposium on Fusion Nuclear Technology (ISFNT-10). doi:https://doi.org/10.1016/j.fusengdes.2011.11.005. URL http://www.sciencedirect.com/science/article/pii/S0920379611006090

[2] L. M. Giancarli, X. Bravo, S. Cho, M. Ferrari, T. Hayashi, B.-Y. Kim, A. Leal-Pereira, J.-P. Martins, M. Merola, R. Pascal, I. Schneiderova, Q. Sheng, A. Sircar, Y. Strebkov, J. van der Laan, A. Ying, Overview of recent ITER TBM program activities, Fusion Engineering and Design 158 (2020) 111674. doi:https://doi.org/10.1016/j.fusengdes.2020.111674. URL http://www.sciencedirect.com/science/article/pii/S0920379620302222

[3] Optimization of Radiation Protection in the Control of Occupational Exposure, no. 21 in Safety Reports Series, International Atomic Energy Agency, 2002. URL https://www.iaea.org/publications/6288/optimization-of-radiation-protection-in-the-control-of-occupati

[4] Comité Européen de Normalisation, Brides et leurs assemblages - Brides circulaires pour tubes, appareils de robinetterie, raccords et accessoires, désignées Class - Partie 1 : Brides en acier NPS 1/2 à 24, Technical standard, NF EN 1759-1 (2005).

[5] Comité Européen de Normalisation, Tubes sans soudure pour service sous pression - Conditions techniques de livraison - Partie 5 : Tubes en aciers inoxydables, Technical standard, NF EN 10216-5 (2014).

[6] AFCEN, Règles de conception et de construction des matériels mécaniques des installations nucléaires hautes températures, expérimentales et de fusion (RCC-MRx), Code (2015).

[7] F. Ledrappier, J.-F. Juliaa, A. Béziat, K. Vulliez, L. Mirabel, M. Wataru, K. Shirai, H.-P. Winkler, R. Hueggenberg, Numerical simulation of HELICOFLEX metallic gasket ageing mechanism for spent fuel cask, in: PATRAM 2016 - The 18th International Symposium on the Packaging and Transportation of Radioactive Materials, Kobe, Japan, 2016. URL https://hal-cea.archives-ouvertes.fr/cea-02439458

[8] ASME, Boiler and Pressure Vessel Code - II: Materials - Part D: Properties (Metric), Code (2010).

[9] B. B. Mikić, Thermal contact conductance; theoretical considerations, International Journal of Heat and Mass Transfer 17 (2) (1974) 205–214. doi:https://doi.org/10.1016/0017-9310(74)90082-9. URL http://www.sciencedirect.com/science/article/pii/0017931074900829

[10] A. P. Colburn, A method of correlating forced convection heat transfer data and a comparison with fluid friction, Vol. 29 of Transactions of the American Institute of Chemical Engineers, American Institute of Chemical Engineers, 1933, pp. 174–209.

[11] H. Petersen, The properties of helium: density, specific heats, viscosity, and thermal conductivity at pressures from 1 to 100 bar and from room temperature to about 1800 K, Report, Danish Atomic Energy Commission (1970). URL http://inis.iaea.org/search/search.aspx?orig_q=RN:02006165

[12] B. Le Neindre, Conductivité thermique des fluides sous pression, Techniques de l'ingénieur Équations d'états et constantes thermiques TIB340DUO (K428). URL https://www.techniques-ingenieur.fr/base-documentaire/sciences-fondamentales-th8/equations-d-etats-et-constantes-thermiques-42340210/conductivite-thermique-des-fluides-sous-pression-k428/